The effect of rotation speed and mixer size on granular flow and mixing in bladed mixers

Angga Herman[1], *Jieqing* Gan[1,*], and *Aibing* Yu[1]

[1]Laboratory of Simulation and Modelling of Particulate System, ARC Hub for Computational Particle Technology, Department of Chemical Engineering, Monash University, Melbourne, VIC 3800, Australia.

Abstract. Bladed mixers are widely used in the industry for granular mixing. In the past decades, the mixing of particles in bladed mixers has been extensively investigated experimentally and numerically. Recently, GPU-based DEM has been employed to simulate various industrial-scale applications. This work aims to apply the GPU-based DEM to investigate the effect of rotation speed and mixer size on granular mixing in bladed mixers of different sizes. The simulation in a larger mixer revealed distinct particle flow patterns that well-describe the mixing mechanism which is difficult to observe in a smaller mixer. The Lacey's mixing index curves revealed a delay in mixing as the mixer size increases. The mixing rate decreases as the mixer size increases and it can be improved with increasing rotation speed. The average particle velocity increase significantly with increasing rotation speed and mixer size.

1. Introduction

The bladed mixer is a typical mixer used in bulk chemicals processing, food, and pharmaceutical industries. Mainly, the bladed mixer is used to homogenize granulate powders, and to enhance a chemical reaction [1]. Inadequate mixing in product manufacturing could cause product rejection due to poor product quality. The mixing process in a bladed mixer has been studied extensively for the past decades. Stewart et al. [2] used the positron emission particle tracking (PEPT) experiment to study the motion of particles in a bladed mixer. They described that the particles moved upwards, forming a heap and eventually, moved over the blade. However, the PEPT experiment lacks dynamic information at the particle scale and can suffer from experimental errors due to low resolution and/or uncertainty in data interpretation [3].

The discrete element method (DEM) simulation can provide microscopic information such as the trajectories, velocities, forces and coordination number, which is difficult to obtain from PEPT experiments. Chandratilleke et al. [4] investigated the effect of blade speed on granular flow and mixing in a bladed mixer by DEM. They reported a new way to study particle mixing at particle scale by using the microscopic coordination number. However, one of the drawbacks of DEM simulation is the intensive computational demand that limits its application to only small scale systems.

Recently, the Graphical Processing Unit (GPU) has been applied to solve DEM models in various scientific and industrial-scale applications [5]. It is reported that the speedup ratio of a single GPU compared to a CPU could increase up to 1000 times depending on the GPU accelerator cards and DEM algorithms [5]. Several large scale GPU-DEM simulations for bladed mixers have been performed over the last decade. For example, Radeke et al. [6] investigated the influence of particle size on mixing statistics (Lacey's mixing index and the relative standard deviation) in a four-bladed mixer by using GPU-based DEM simulation. The parallelization performance of 7680 to 7.68 million particles on a single GPU is also compared. However, little effort has been made to compare the impact of operating conditions such as the rotation speed and mixer size on the granular flow and mixing.

In this work, we focus on the effect of rotation speed and mixer size on the flow and mixing of particles in bladed mixers. The mixing flow patterns are presented to qualitatively examine the particle structure during mixing. The mixing performances are quantitatively analysed by using Lacey's mixing index and mixing rate. Finally, microscopic information such as the average particle velocity and the contact forces network is also discussed.

2 Simulation methods and conditions

2.1 DEM governing equations

The particles in a particulate system can experience translational and rotational motion as described by Newton's second law of motion. In general, a particle i with the radius R_i, mass m_i, and moment of inertia I_i, can be described as:

*Corresponding author: jieqing.gan@monash.edu

A video is available at https://doi.org/10.48448/9ps4-2h21

$$m_i \frac{d\boldsymbol{v}_i}{dt} = \sum_{j=1}^{k_c} \left(\boldsymbol{f}_{c,ij} + \boldsymbol{f}_{d,ij}\right) + m_i \boldsymbol{g}, \quad (1)$$

and

$$I_i \frac{d\boldsymbol{\omega}_i}{dt} = \sum_{j=1}^{k_c} \left(\boldsymbol{M}_{t,ij} + \boldsymbol{M}_{r,ij}\right), \quad (2)$$

where $\boldsymbol{v}_i$ and $\boldsymbol{\omega}_i$ represent the translational and angular velocities of the particles, while k_c is the number of particles in interaction with particle i.

The forces involved are $\boldsymbol{f}_{c,ij}$, $\boldsymbol{f}_{d,ij}$ and $m_i\boldsymbol{g}$ which represent the elastic force, viscous damping force and gravitational forces respectively. The torque acting on particle i in contact with particle j can be divided into two components which include $\boldsymbol{M}_{t,ij}$ and $\boldsymbol{M}_{r,ij}$. $\boldsymbol{M}_{t,ij}$ is known as rotation torque which is generated by the tangential force that causes the particle to rotate. Meanwhile, $\boldsymbol{M}_{r,ij}$ is commonly known as a rolling friction torque which is generated by asymmetric normal forces between particles, causing restriction in rotation between particles.

2.2 Mixing performance

The mixing performance of a binary particle mixture in this study is analysed using Lacey's mixing index, M. The evolution of Lacey's mixing index starts at a fully segregated state, 0 and ends in a perfect mixing state, 1. The Lacey's mixing index can be defined by [7]:

$$M = \frac{\left(S_0^2 - S^2\right)}{\left(S_0^2 - S_r^2\right)}, \quad (3)$$

Here, the mono-sized spherical particles are coloured into two different colours, namely red and blue. s_o^2 represents the variance of the fraction of red particles in the binary system in a fully segregated state which is given by $s_o^2 = pq$, where p and q are the proportions of the two different components from the samples. In this work, the sampling size is set to $4d_p$. $s_r^2 = pq/N$ represents the variance of the red particles in sample size N at a fully random mixing state in the binary system, while s^2represents the actual sample variance of the binary system.

The general trend of Lacey's mixing index can be well described mathematically by the function below [8]:

$$M_t = M_e + (M_o - M_e)\, exp(-kt), \quad (4)$$

where M_o represents the initial mixing index, M_e represents the index at steady-state mixing, k, represents the overall mixing rate of the mixing process and t represents the mixing time. The mixing rate, k is obtained by fitting the simulation data into Eq. (4).

2.3 Simulation conditions

In this study, the mixing simulation is performed by using the GPU-based DEM [5]. Four bladed mixers of different sizes, namely: 4.87 L (Mixer A), 38.96 L (Mixer B), 131.48 L (Mixer C) and 311.65 L (Mixer D) are considered. The bladed mixer, Mixer A, has a similar design to that of the bladed mixer used previously in DEM simulations [4]. The fill level is kept constant at 40 % at all time. The particles used in this study increase from 18,400 to 1,180,000 and the mixing performances are evaluated at the rotation speed of 10 RPM, 20 RPM, 50 RPM and 100 RPM, respectively.

The particles used in this study are spherical with the properties similar to glass beads of a diameter 5 mm with a density of 2500 kg/m^3. The physical properties used in the simulation are listed as follows: Poisson's ratio, ν = 0.3, sliding friction coefficient, μ_s = 0.3, rolling friction coefficient, μ_r = 0.00005 m, Young's modulus, E = 2.16 × 10^6 N/m^2 and time step, Δt = 1.129 x 10^{-5} s. The physical properties of the bladed mixer wall are assumed to be the same as those of the particles at all times. The simulation starts with the random generation of spherical particles into the mixer. The particles are generated continuously until it reaches 40 % of the mixer fill level, followed by the gravitational settling for 0.5 s. Initially, both red and blue particles are separated equally by the blades. The simulation starts immediately for at least 25 s to allow the mixing process to reach steady-state.

3 Results and discussions

The mixing flow patterns of the binary particles in bladed mixers of different sizes are investigated. Fig.1 shows the comparison of the temporal evolution of the mixing flow pattern for Mixer A and Mixer D at 10 RPM. From Fig. 1 (ii), the particles in Mixer D are being displaced in groups by the moving blade at 1 s of mixing. The movement of the blades pushes the particles upward to form the heap. Later, the particles fall over the blades and form layers of particles of different colours as the mixing progresses to 15 s of mixing. After that, the layers of different colours start to disperse as the particles start to move individually instead of in their respective groups, as shown in Fig.1 (ii) (d). At 50 s of mixing, the initially segregated particles nearly achieve homogeneous mixing. Unlike Mixer D, Mixer A can achieve homogeneous mixing at 25 s of mixing.

The mixing performances can be evaluated by using Lacey's mixing index as expressed by Eq. (3). Fig.2 illustrates the evolution of Lacey's mixing index as a function of time or blade revolution at 10 RPM. It can be observed that the mixing index curves increase gradually, indicating that the initially segregated particles are displaced slowly in groups by the moving blades. At 10 RPM, the mixing index curves are unable to reach a plateau, demonstrating that the particles failed to achieve homogeneous mixing after 25 s of mixing for all mixers. It is mainly due to a low convective movement caused by the moving blades as a result of low rotation speed. The mixing at 10 RPM is then extended to 50 s of mixing and even though it is not shown here, the mixing index curves can reach a plateau after approximately 45 s of mixing for Mixer A, Mixer B, Mixer C and Mixer D, respectively.

Conversely, the mixing index curves increase sharply for a short amount of time before reaching a plateau at a high rotation speed. Fig.3 shows Lacey's mixing index

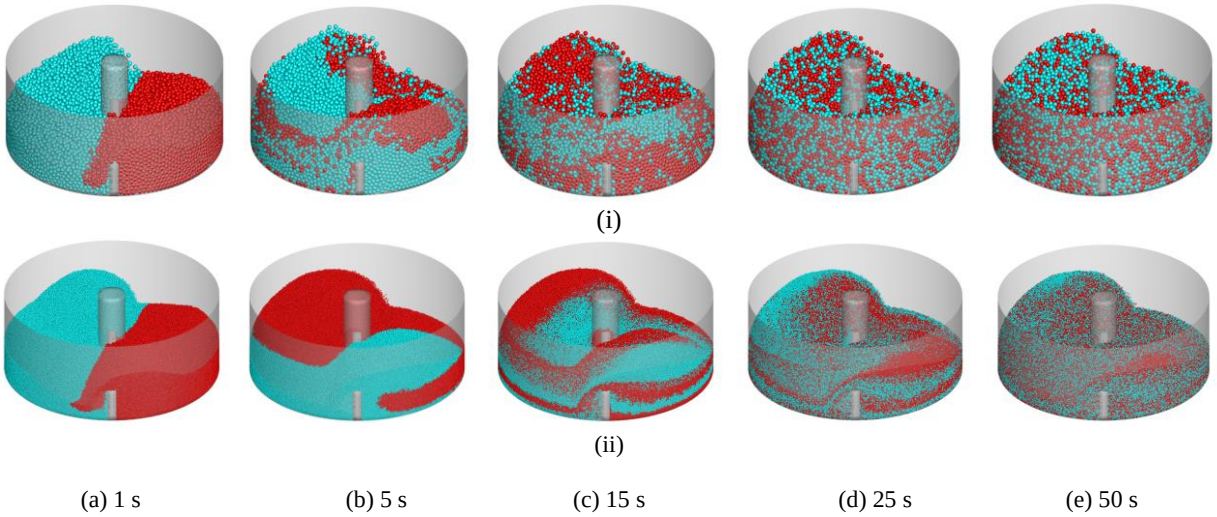

Fig.1: The comparison for the evolution of the particle flow pattern at 10 RPM for (i) Mixer A, and (ii) Mixer D at (a) 1 s, (b) 5 s, (c) 15 s, (d) 25 s, (e) 50 s of mixing time.

curves as a function of time or blade revolution at 50 RPM. It can be observed that the Mixer A, Mixer B, Mixer C, and Mixer D achieve steady-state mixing after approximately 5 s, 8 s, 10 s and 16 s of mixing, respectively. At high rotation speed, the particles experience a high convective movement caused by the moving blades, causing a rapid displacement of the particles. A shorter mixing time is required as the rotation speed increases, but a longer mixing time is required for the larger mixer to achieve similar mixing quality as the smaller mixer. A large number of particles in a larger mixer causes the particles of different colours to relocate themselves in a larger space, subsequently causing a slight delay in mixing. Moreover, the steady-state value of Lacey's mixing index for all mixers is similar at the end of 25 s of mixing.

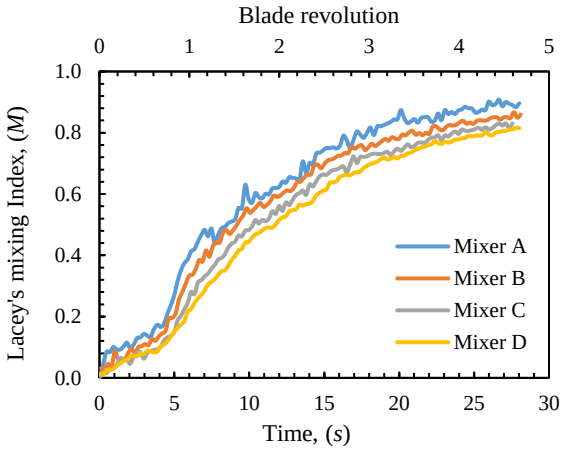

Fig.2: The evolution of Lacey's mixing index, *M* as a function of time or blade revolution for all mixers at 10 RPM.

The mixing rate defines how quickly the initially segregated particles become homogeneous, which can be described mathematically by using Eq. (4). Fig.4 depicts the semi-log curves of the mixing rate as a function of rotation speed and mixer size. It can be observed that the mixing rate decreases as the mixer becomes larger. Particularly at a higher rotation speed, a significant change of mixing rate is observed. It is mainly because to that a large number of particles are displaced in a short amount of time by the blades at a higher rotation speed. However, a large number of particles in a larger mixer causes the particles relocation to be more difficult, subsequently leading to a delay in mixing. This can be clearly seen in the mixing index curves in Figs. 2 and 3, respectively.

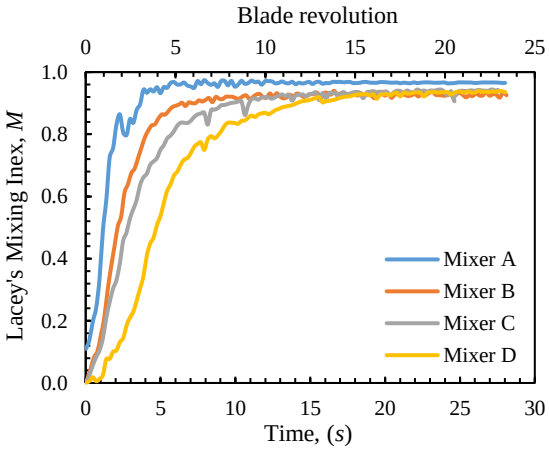

Fig.3: The figure of Lacey's mixing index, *M* for 30 s of mixing at 50 RPM for all mixers.

DEM simulations can provide microscopic information such as the particle velocity within a particulate system. Fig. 5 shows the average particle velocity at steady-state as a function of mixer sizes and rotation speed. The average particle velocity increases with rotation speed. It is mainly due to the particles experience higher velocity at a higher rotation speed. In addition to that, the average particle velocity also increases significantly at a constant rotation speed. It is

mainly due to that the blade tip speed increases as the mixer size increases. As a result, the particles in the larger mixer will experience higher average particle velocity, as compared to the particles in the smaller mixer.

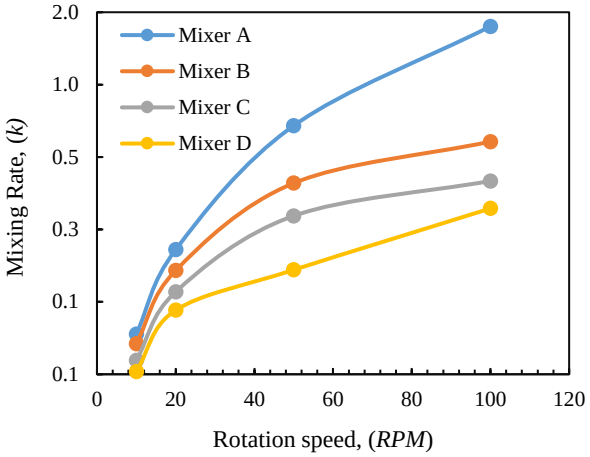

Fig.4: The relationship between the mixing rate and mixer sizes at a different rotation speed.

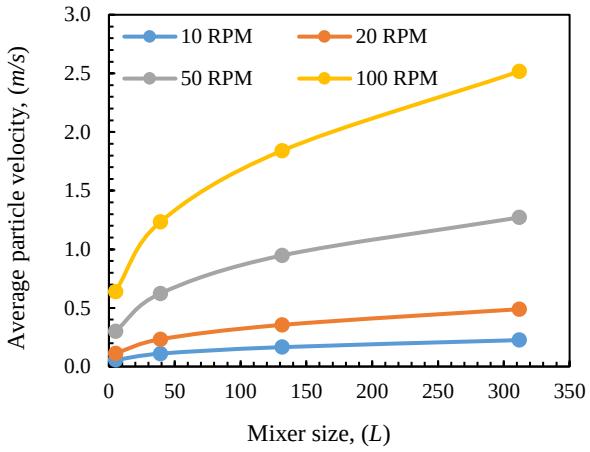

Fig.5: The average particle velocity at steady-state as a function of rotation speed and mixer sizes.

The effect of mixer size on the interparticle contact forces network at a constant rotation speed is also investigated. Fig. 6 shows the comparison of the contact forces network of Mixer A and Mixer D at 10 RPM from the bottom view. Note that the mixer is sliced at Y > 0 to display only half of the mixer. The contact forces network is represented by a line that connects the centre of two contacting particles. Meanwhile the thickness and colours represent the magnitude of the contact forces network. It can be observed that a large contact forces network is focused near the bottom corner of the moving blade. The contact forces network becomes weaker as the particles are away from the moving blades. It is also observed that the contact forces network for Mixer D is denser as compared with that of Mixer A.

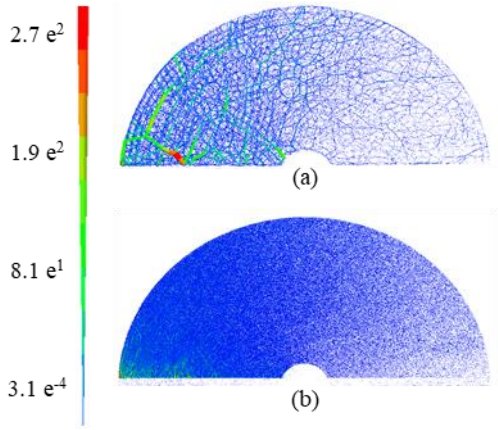

Fig.6: The contact force network diagram from the bottom view for (a) Mixer A, and (b) Mixer D at 10 RPM. (unit: N)

4. Conclusions

This study highlighted the importance of a large-scale simulation in the means of GPU-based DEM which allows us to understand the effect of rotation speed and mixer size on flow and mixing of particles in bladed mixers. Large mixer size revealed clear layers of different colours as the particles are displaced by the moving blades. These layers will disperse as the mixing progresses. Lacey's mixing index curves showed that the mixing is delay as the mixer becomes larger and the mixing rate can be improved with increasing rotation speed. The average particle velocity increases when the rotation speed and mixer size increase. This study lays a groundwork for future development that aims to address scale-up problems in different mixers.

The authors want to acknowledge the Australian Research Council (ARC) Hub for Computational Particle Technology (ARC IH140100035) for the financial support of this work, and the Monash MASSIVE GPU clusters for the support in computation.

References

[1] A. Lekhal, S. L. Conway, B. J. Glasser, and J. G. Khinast, AlChE J., **52**, 2757-2766, (2006)
[2] R. L. Stewart, J. Bridgwater, and D. J. Parker, Chem. Eng. Sci., **56**, 4257-4271, (2001)
[3] R. L. Stewart, J. Bridgwater, Y. C. Zhou, and A. B. Yu, Chem. Eng. Sci., **56**, 5457-5471, (2001)
[4] G. R. Chandratilleke, Y. C. Zhou, A. B. Yu, and J. Bridgwater, Ind. Eng. Chem. Res., **49**, 5467-5478, (2010)
[5] J. Q. Gan, Z. Y. Zhou, and A. B. Yu, Powder Technol., **301**, 1172-1182, (2016)
[6] C. A. Radeke, B. J. Glasser, and J. G. Khinast, Chem. Eng. Sci., **65**, 6435-6442, (2010)
[7] P. M. C. Lacey, J. Appl. Chem., **4**, 257-268, (1954)
[8] P. Y. Liu, R. Y. Yang, and A. B. Yu, Granul. Matter, **15**, 427-436, (2013)